

Cosmic-ray cooling in active galactic nuclei as a new probe of inelastic dark matter

R. Andrew Gustafson^{1,2,*}, Gonzalo Herrera^{1,†}, Mainak Mukhopadhyay^{3,‡},
Kohta Murase^{3,4,§} and Ian M. Shoemaker^{1,||}

¹Center for Neutrino Physics, Department of Physics, *Virginia Tech*,
Blacksburg, Virginia 24061, USA

²International Center for Quantum-field Measurement Systems for Studies of the
Universe and Particles (QUP,WPI), *High Energy Accelerator Research Organization (KEK)*,
Oho 1-1, Tsukuba, Ibaraki 305-081, Japan

³Department of Physics, Department of Astronomy and Astrophysics,
Center for Multimessenger Astrophysics, Institute for Gravitation and the Cosmos,
The Pennsylvania State University, University Park, Pennsylvania 16802, USA

⁴Center for Gravitational Physics and Quantum Information, *Yukawa Institute for Theoretical Physics*,
Kyoto, Kyoto 606-8502 Japan

 (Received 4 September 2024; revised 24 March 2025; accepted 4 June 2025; published 25 June 2025)

We present a novel way to probe inelastic dark matter using cosmic-ray (CR) cooling in active galactic nuclei (AGNs). Dark matter (DM) in the vicinity of supermassive black holes may scatter off CRs, resulting in the rapid cooling of CRs for sufficiently large cross sections. This in turn can alter the high-energy neutrino and gamma-ray fluxes detected from these sources. We show that AGN cooling bounds obtained through the multimessenger data of NGC 1068 and TXS 0506 + 056 allows us to reach unprecedentedly large mass splittings for inelastic DM ($\gtrsim \text{TeV}$), orders of magnitude larger than those probed by direct detection experiments and DM capture in neutron stars. Furthermore, we demonstrate that cooling bounds from AGNs can probe thermal light DM with small mass splittings. This provides novel and complementary constraints in parts of a parameter space accessible solely by colliders and beam-dump experiments.

DOI: [10.1103/5m57-vgt2](https://doi.org/10.1103/5m57-vgt2)

Introduction. A pressing problem in high-energy physics and cosmology resides in the yet unknown nature of dark matter (DM), confirmed only via its gravitational effects on visible matter [1]. In the current paradigm, the DM is believed to likely be composed of one or more fundamental particles that couple weakly or feebly to the Standard Model (SM) sector [2–4].

An early proposal to search for weakly interacting massive particles accounting for the observed DM abundance of the Universe, dubbed direct detection, consists in looking for its scatterings off nuclei at Earth-based detectors [5,6]. In some DM models, the inelastic scattering

channel can naturally dominate over the elastic one [7–15]. In this scenario, DM with mass m_{DM} upscatters with SM particles to an excited (heavier) state with mass m_{DM}^* , where $m_{\text{DM}}^* = m_{\text{DM}} + \delta_{\text{DM}}$ and δ_{DM} is defined as the mass splitting. A canonical example is the vector current of Majorana DM, which is forbidden for the elastic case but not for the inelastic one. Indeed, for a Majorana fermion ψ ,

$$\bar{\psi}\gamma_{\mu}\psi = \bar{\psi}^c\gamma_{\mu}\psi^c = -\bar{\psi}\gamma_{\mu}\psi, \quad (1)$$

since for a Majorana field the charge conjugation operation leaves the field unchanged $\psi^c = \psi$. The off-diagonal current between two nondegenerate Majorana fields, could, however, be nonzero (see Supplemental Material [16] for a discussion on concrete realizations of inelastic DM [8,17–19]).

Such inelastic DM models are only weakly constrained by direct detection experiments, reaching maximum mass splittings between the two DM states of order ~ 100 keV, e.g., Refs. [8,20–28], and are largely unconstrained by direct detection for sub-GeV DM masses, e.g., Refs. [17,25,29–34]. Furthermore, it should be noted that indirect (astrophysical) constraints on inelastic DM restrict to some regions of parameter space only (and rely on future

*Contact author: gustafr@vt.edu

†Contact author: gonzaloherrera@vt.edu

‡Contact author: mkm7190@psu.edu

§Contact author: murase@psu.edu

||Contact author: shoemaker@vt.edu

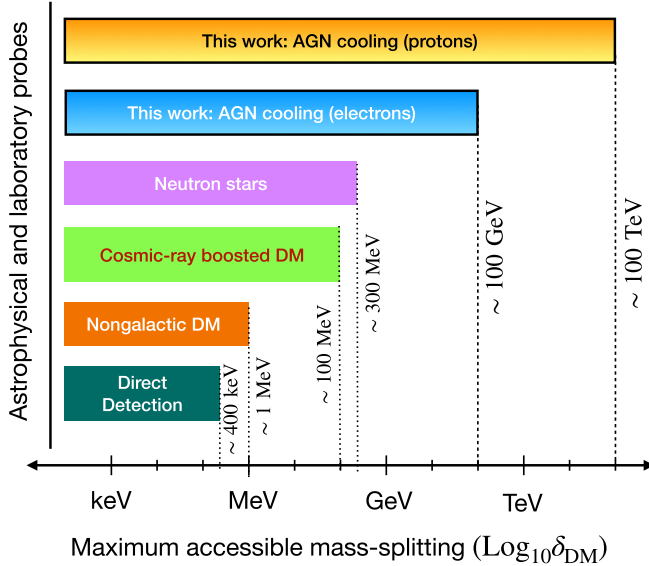


FIG. 1. Maximum mass splitting of inelastic DM reached by various astrophysical and laboratory probes: direct detection of DM from the galactic halo [23], direct detection of a nongalactic high-speed DM component [25], direct detection of CR-boostered DM [24], DM capture in neutron stars [35], and CR cooling in AGN (this work). The cooling of CRs in AGN, inferred from multimessenger high-energy neutrino and electromagnetic observations, allows us to reach the largest mass splittings of inelastic DM to date.

observations of nearby neutron stars), e.g., Refs. [35–42], or probe self-annihilations of DM particles, but lack in probing signatures arising from scatterings [43].

In some regions of parameter space, focused particularly on comparable masses of the DM and the particle mediating the interaction between the DM and the SM (“mediator” hereafter), colliders and fixed-target experiments can produce strong constraints on a dark sector mediator, e.g., Refs. [17,44,45]. While collider constraints provide complementary constraints to direct detection and astrophysical probes, they cannot probe particles with cosmological lifetimes nor the distribution of DM in the Universe. Besides, previous analyses have not been assessed for sub-MeV DM masses nor have studied large ratios between the DM mass and the mass splitting.

Here we propose the cooling of cosmic rays (CRs) from some active galactic nuclei (AGN), inferred from combined electromagnetic (EM) and high-energy neutrino observations, as a probe of inelastic DM across orders of magnitudes in DM mass, mediator mass and mass splitting. Reference [46] demonstrated that light DM in the vicinity of the black hole scattering off CR protons and electrons can cool them in such environments, affecting their multimessenger emissions. The impact of light DM-CR scatterings on only the electromagnetic emission from the nuclei of starburst galaxies was also considered in Ref. [47]. We will demonstrate here that DM-proton and DM-electron

upscattering the DM to an excited state can also allow one to constrain inelastic DM, probing new regions of parameter space and filling gaps in current constraints obtained with complementary probes such as direct detection and collider experiments. See Fig. 1 for a visual representation of the reach of AGN compared to other inelastic dark matter probes.

CR cooling timescales in AGN. CR protons and electrons can be efficiently accelerated in the vicinity of a central supermassive black hole through shocks, turbulence or magnetic reconnections. Plausible acceleration sites include disk coronae and jets [48]. The accelerated CR protons then interact with the protons or the photons in the respective regions to produce neutrinos and EM signatures through pp and $p\gamma$ processes [49]. The CR protons also cool through various other SM processes like synchrotron, inverse Compton, Bethe-Heitler pair production processes and adiabatic losses. Furthermore, the escape of CR protons or electrons from the sources is quantified by advection or diffusion. For NGC 1068 and TXS 0506 + 056, detailed multimessenger data and modeling are available, enabling us to evaluate the energy dependence of cooling times. This allows us to constrain DM properties only via bolometric luminosities without relying on intrinsic spectra of astrophysical neutrinos that are currently uncertain.

CR protons in NGC 1068 are cooled at high energies mainly via pp , $p\gamma$ and Bethe-Heitler interactions ($N\gamma \rightarrow N^*e^-e^+$, with N and N^* the initial and final nuclei) [50]. Concretely, at energies below $T_p \lesssim 10^4$ GeV, the dominant cooling process is pp interactions with ambient gas. At energies in between $T_p \sim 10^4$ and 10^6 GeV, the Bethe-Heitler production mechanism becomes relevant, and at energies above $\sim 10^6$ GeV, $p\gamma$ interactions are responsible for CR energy losses [51]. In TXS 0506 + 056, CR electrons are mainly cooled by inverse Compton scattering, synchrotron radiation, and escape losses [52]. At energies below $T_e \lesssim 5$ GeV, escape losses dominate. At energies between ~ 5 and 40 GeV, inverse Compton scattering becomes relevant, and at energies above ~ 40 GeV, synchrotron radiation becomes the main cooling mechanism of CR electrons. The behaviors of the cooling timescales with the CR energy for both NGC 1068 and TXS 0506 + 056 are manifest in Fig. 2.

In general, the SM cooling processes and timescales for astrophysical sources are model dependent. However, for TXS 0506 + 056 and NGC 1068, the multimessenger spectral energy distributions are available, enabling us to evaluate these timescales and derive conservative bounds on DM-SM interactions.

Cooling timescales induced by inelastic DM-proton and DM-electron interactions. Neutrino and gamma-ray observations allow us to constrain the CR cooling induced by DM-proton and DM-electron scatterings [46]. The cooling

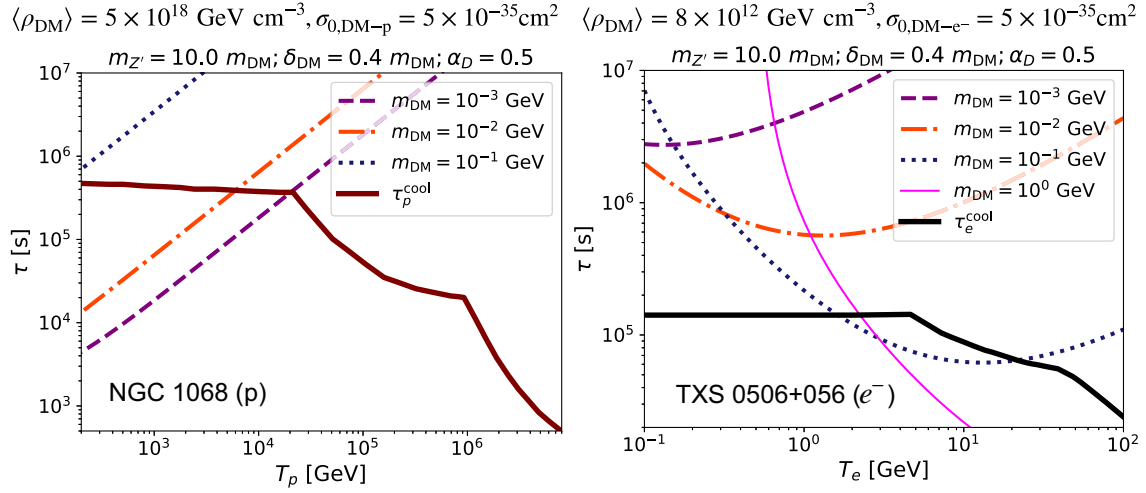


FIG. 2. Cooling timescales from CR protons (left) and electrons (right) scattering with inelastic DM, compared with those from SM processes [51]. We take the average dark matter density obtained from a spike formed in the region of cosmic-ray acceleration $\langle\rho_{\text{DM}}\rangle$ (see Supplemental Material [16] for details) and fix the nonrelativistic scattering cross section to $\sigma_{0,\text{DM-p}} = 5 \times 10^{-35} \text{ cm}^2$. We fix the mass splitting among the two dark matter states as $\delta_{\text{DM}} = 0.4 m_{\text{DM}}$, fix the mediator mass as $m'_Z = 10 m_{\text{DM}}$, and sample for different values of the dark matter mass m_{DM} . Furthermore, we use a benchmark value of the dark structure constant, $\alpha_D = g_{\text{DM}}^2/4\pi = 0.5$. For the case of proton cooling, we see that the timescales become larger as m_{DM} increases (i.e., as the number density decreases). The timescales also increase with T_p since scattering becomes ineffective at large-momenta transfers. For the case of electron scattering, we see that cooling timescales initially decrease with T_e and then start to increase once $2m_{\text{DM}}T_e - \delta_{\text{DM}}^2 \gtrsim m_{Z'}^2$.

timescale due to inelastic DM-SM scatterings is given by

$$\frac{dE}{dt} = -\frac{\langle\rho_{\text{DM}}\rangle}{m_{\text{DM}}} \int_{T_{\text{DM}}^{\min}}^{T_{\text{DM}}^{\max}} dT_{\text{DM}} (T_{\text{DM}} + \delta_{\text{DM}}) \frac{d\sigma_{\text{DMSM} \rightarrow \text{DM}^* \text{SM}}}{dT_{\text{DM}}}, \quad (2)$$

where $\langle\rho_{\text{DM}}\rangle$ is the average DM density in the vicinity of the supermassive back hole at the center of an AGN, where scatterings are more likely to occur. We refer the reader to Supplemental Material [16] Secs. S3 and S4 for details on the above equation and $\langle\rho_{\text{DM}}\rangle$ with adiabatic spike formation, respectively [25,46,53–56]. The energy loss rate induced by inelastic DM-proton and DM-electron scatterings can be translated into a cooling timescale of these interactions, which reads

$$\tau_{\text{DM-SM}}^{\text{inel}} = \left[-\frac{1}{E} \left(\frac{dE}{dt} \right) \right]^{-1}. \quad (3)$$

In Fig. 2, we show the cooling timescales induced DM-proton (electron) interactions¹ in NGC 1068 (TXS 0506 + 056), for different values of the DM mass and mass splitting between the two DM states and fixed benchmark values of the characteristic cross section. For comparison, we show the cooling timescales induced by SM processes in these sources, inferred from multimessenger observations. It can be appreciated that for certain values of the

inelastic DM parameters, the cooling timescales can be comparable to or shorter than the SM cooling timescales at the relevant energies, which would contradict observations on Earth. Concretely, we can derive an upper limit on the inelastic DM-proton and DM-electron scattering cross section from the requirement

$$\tau_{\text{DM-SM}}^{\text{inel}} \geq C \tau_{\text{SM}}^{\text{cool}}, \quad (4)$$

where C is a model- and source-dependent factor. We use $C = 0.1$ and $C = 1$ for NGC 1068 and TXS 0506 + 056, respectively, to derive constraints in this work. We explain this choice in detail in Supplemental Material [16,51,52,57–60]. Briefly, this criterion is consistent with the energetics requirement from multimessenger observations of AGN. For NGC 1068, the CR proton luminosity would be $10^{43} \text{ erg s}^{-1} \lesssim L_p \lesssim L_X \lesssim \text{a few} \times 10^{44} \text{ erg s}^{-1}$ [51,57], justifying $C \sim 0.1$ – 1 , where L_X is the total (bolometric) luminosity. For TXS 0506 + 056, the absolute proton luminosity in the single-zone model would violate the Eddington luminosity L_{Edd} [60], so our choice is conservative for protons. This is also reasonable for electrons. The total isotropic equivalent electron luminosity is $L_e \sim 8 \times 10^{47} \text{ erg s}^{-1}$, in which the absolute electron luminosity can be lower than L_{Edd} [52]. For NGC 1068, we consider proton energies 10–300 TeV to place constraints, while for TXS 0506 + 056 we consider electron energies 50 GeV–2 TeV. We note that as m_{DM} increases, the number of DM particles decrease since $\langle\rho_{\text{DM}}\rangle$ is fixed leading to higher timescales or lower rates. Thus better constraints can be obtained for lighter DM masses. In fact, we see, for

¹For NGC 1068 we do not have significant evidence for electron acceleration and for TXS 0506 + 056 proton acceleration gives weaker bounds than NGC 1068.

$m_{\text{DM}} \sim 10^{-3}$ GeV, the DM-induced cooling dominates the SM cooling channels for $T_p < \text{a few} \times 10^4$ GeV. We note that, in our model, the upscattered dark matter state may decay into the lightest state plus Standard Model particles, which may reinject energy into the Standard Model sector affecting nontrivially the electromagnetic spectrum. We considered the decay $\chi_2 \rightarrow \chi_1 + \gamma$. While this decay is forbidden at the tree level due to gauge invariance (see our dedicated discussion in Supplemental Material [16]), it may occur via a dipole operator. Assuming this operator is large enough for the decay to occur on sufficiently small time-scales, we estimate the energy transfer into the SM sector to be $1/2$ or less for cosmic-ray protons but could be larger for cosmic-ray electrons for same combinations of dark matter mass and mass splittings in the dark sector. For the scenario where dark matter cools cosmic-ray protons, the energy loss from the scattering will have a direct impact on the energy and flux of resulting high-energy neutrinos, which is a sufficient condition to place our constraints from TXS 0506 + 056 and NGC 1068 given IceCube data. For dark matter interactions with cosmic-ray electrons, however, the modification of the low-energy gamma-ray flux due to decays of the upscattered state may lead to degeneracies with the expected low-energy gamma-ray flux from competing SM processes like electron-positron annihilation, synchrotron radiation or inverse Compton scattering, among others. A calculation of the modified fluxes and their comparison with electromagnetic observations would allow us to refine the ensuing limits derived from cooling arguments in this work.

Upper limits on inelastic DM-proton and DM-electron interactions. By means of Eq. (4), we can derive upper limits on the scattering cross section of inelastic DM off nucleons and electrons. Our model has five free parameters: the lighter state DM mass m_{DM} , the mass splitting between the DM states δ_{DM} , mediator mass $m_{Z'}$ and couplings of the mediator to the SM sector, g_{SM} , and to the dark sector g_{DM} .

We will derive constraints in this multidimensional parameter space in two distinct and physically motivated regimes. First, we will focus on the parameter space corresponding to a fixed relation between the mediator and DM masses ($m_{Z'} = 10m_{\text{DM}}$ and $m_{Z'} = 3m_{\text{DM}}$) and to a fixed relation between the DM mass and the mass splitting ($\delta_{\text{DM}} = 0.4m_{\text{DM}}$ and $\delta_{\text{DM}} = 0.8m_{\text{DM}}$). Furthermore, we will fix the dark gauge coupling to a “natural” value ($\alpha_D = 0.5$). Such relations between inelastic DM parameters have been discussed previously in the literature, e.g., Refs. [17,44,45,61,62]. It has been shown that for light (MeV-scale) DM, such relations predict a thermal relic that can be within reach of collider and beam-dump experiments. Here we will demonstrate that this region of parameter space can also be probed by CR cooling in AGN.

In Fig. 3 we show constraints in the previously discussed parameter space, from CR proton cooling in NGC 1068 (dark blue) and CR electron cooling in TXS 0506 + 056 (light blue), for asymmetric or weakly self-annihilating DM (solid) and for a sizable DM self-annihilation cross section ($\langle\sigma v\rangle/m_{\text{DM}} = 10^{-28} \text{ cm}^3 \text{ s}^{-1}/\text{GeV}$ for TXS 0506 + 056, $\langle\sigma v\rangle/m_{\text{DM}} = 10^{-31} \text{ cm}^3 \text{ s}^{-1}/\text{GeV}$ for NGC 1068), which depletes the distribution to a core in these sources. In the

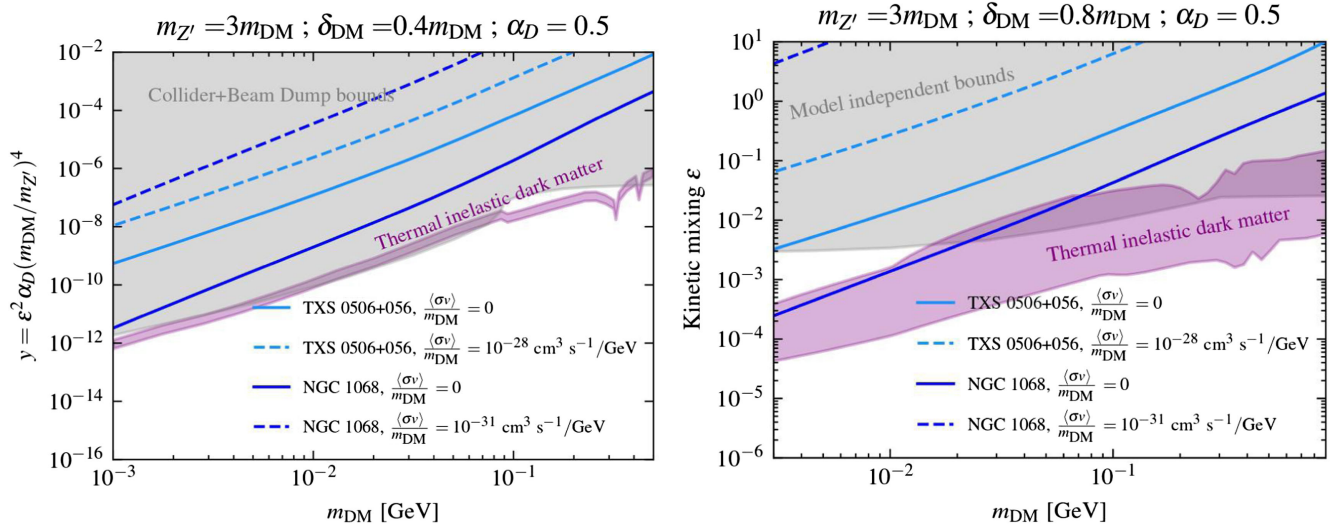


FIG. 3. Left: AGN cooling constraints on the DM-proton and DM-electron interaction strength, parametrized as y . Solid lines show constraints when considering the dark matter density at the cosmic-ray acceleration regions arising from a spike, while dashed lines correspond to the density expected from a cored profile (see Supplemental Material [16] for details). For comparison, we show constraints from collider and beam-dump experiments, and combination of values able to account for thermal DM, from [17,45]. Right: AGN cooling constraints on the kinetic mixing ϵ vs the mass of the DM m_{DM} , for fixed relations $m_{Z'} = 3m_{\text{DM}}$, $\delta_{\text{DM}} = 0.8m_{\text{DM}}$, and $\alpha_{\text{DM}} = 0.5$. For comparison, we show model-independent constraints from collider and beam-dump experiments and thermal DM targets from [17]. To derive these constraints, we consider the cooling of cosmic rays in the following energy ranges: 30–100 TeV for NGC 1068 and 0.1–20 PeV for TXS 0506 + 056 (see main text for details).

left plot, we constrain the quantity $y = \epsilon^2 \alpha_D (m_{\text{DM}}/m_{Z'})^4$ in which $\epsilon = g_{\text{SM}}/e$, to allow for comparison with existing literature. We show a band of thermal inelastic light DM. The upper end of the band has been derived in various works, e.g., Refs. [17,44,45,62], while the range of values extending to the lowest end was derived in Ref. [17]. These correspond to different plausible values of the dark left-right coupling asymmetry ($\sim y_L - y_R$) or Majorana mass asymmetry ($\sim m_L - m_R$), which are common parameters in concrete models of inelastic DM. This parameter quantifies the asymmetry in the Lagrangian terms $\mathcal{L}_\chi \supset -\frac{1}{2} m_L \bar{\chi}_L^c \chi_L - \frac{1}{2} m_R \bar{\chi}_R^c \chi_R$ or $\mathcal{L}_\chi \supset -\sqrt{2} y_L S \bar{\chi}_L^c \chi_L - \sqrt{2} y_R S \bar{\chi}_R^c \chi_R$, where S is a singlet scalar and $\chi_{L,R}$ are the left and right DM field components, respectively [17] (see Supplemental Material [16] for details). Concretely, denoting the asymmetry as $\delta_y \equiv (y_R - y_L)/y_L = (m_R - m_L)/m_L$, we use values in the range from $\delta_y = 0$ –1000.

Furthermore, we show in gray a combination of collider and beam-dump experiment constraints in these models. For the chosen combination of inelastic DM parameters, our cooling constraints can be stronger than collider constraints for masses below $m_{\text{DM}} \sim 1$ MeV, probing thermal values.

In the right panel of Fig. 3, we show constraints derived for different values of the mediator and DM mass ratio and mass splitting. In this case, it can be appreciated that our cooling constraints can be stronger than the (model-independent) collider and beam-dump experimental constraints for masses below $m_{\text{DM}} \lesssim 20$ MeV and allow us to probe thermal inelastic DM for masses below $m_{\text{DM}} \lesssim 70$ MeV.

Notably, our limits on y and ϵ become stronger at light DM masses. This is because, first, the number density of DM particles in the AGN increases for light DM masses, which increases the probability of interactions. Second, the scattering cross section of inelastic DM off electrons and protons in these environments increases at low DM masses, due to the inverse dependence with the reduced mass of the DM-proton and DM-electron systems; confer Eq. (S8) [16]. The enhanced cross section induces shorter cooling time-scales at low DM masses and, thus, stronger bounds on the interaction strength.

The parameter space discussed previously, although predictive, is narrow and may misrepresent the actual relations between the DM mass and the mediator mass and between the DM mass and the size of the mass splitting. Therefore, in the following we present more general constraints in the parameter space spanned by the DM mass, the mass splitting, and the interaction strength of the DM with the SM sector. We will derive constraints in the limit where the mediator mass of the interaction is much heavier than the momentum transfer of the scattering process in the AGN, and we will present our constraints on the nonrelativistic scattering cross section as defined in Eq. (S7) [16].

Moreover, we present analogous constraints in the limit of a finite mediator mass ($m_{Z'} = 10$ MeV) and show contours for limits on the product of the gauge couplings

instead of the nonrelativistic cross section. It should be noticed that in some regions of the displayed parameter space, particularly at high DM masses, the cooling constraints are very weak; i.e., it may be difficult to interpret them physically since the cross sections and couplings probed are nonperturbative. A detailed discussion on this regard can be found in Supplemental Material [16].

Our results are summarized in Fig. S8 [16]. We show contour constraints on the parameter space of DM mass, mass splitting and scattering cross section, for TXS 0506 + 056 (left panels) and NGC 1068 (right panels). We see that cross section bounds become weaker as the DM mass increases (and thus the number density decreases). The bounds become stronger as δ_{DM} increases because q^2 decreases at larger δ_{DM} , giving less suppression to the differential cross section as seen in Eq. (S8) [16]. This effect is even more pronounced for protons, even in the heavy mediator limit, as the form factor decreases with larger q^2 . We know that cooling is only possible when $s > (m_{\text{SM}} + m_{\text{DM}} + \delta_{\text{DM}})^2$, which is why bounds become weaker when $m_{\text{DM}} \lesssim (\delta_{\text{DM}}^2 + 2m_{\text{SM}}\delta_{\text{DM}})/(2T_{\text{SM,min}} - 2\delta)$ and completely go away when $m_{\text{DM}} \lesssim (\delta_{\text{DM}}^2 + 2m_{\text{SM}}\delta_{\text{DM}})/(2T_{\text{SM,max}} - 2\delta_{\text{DM}})$, where $T_{\text{SM,min}}$ ($T_{\text{SM,max}}$) is the minimum (maximum) electron or proton kinetic energy considered for cooling.

Inelastic DM has also been explored in the context of direct detection experiments and interactions with compact celestial objects like white dwarfs and neutron stars. In these cases, we may define the kinematic requirement for scattering to be

$$m_{\text{DM}}^2 + m_{\text{SM}}^2 + 2 \frac{m_{\text{DM}} m_{\text{SM}}}{\sqrt{1 - v_{\text{rel}}^2}} > (m_{\text{SM}} + m_{\text{DM}} + \delta_{\text{DM}})^2, \quad (5)$$

where v_{rel} is the velocity of the DM particle in the rest frame of the SM particle. A detailed analysis of these methods would consider the full velocity distributions of DM and SM particles. For now, we will simply take characteristic relative velocities of $v_{\text{rel}} = 10^{-3}$ for direct detection and $v_{\text{rel}} = 0.8$ for neutron stars and white dwarfs. This can be translated into a requirement on the mass splitting of

$$\delta_{\text{DM}} \leq -m_{\text{SM}} - m_{\text{DM}} + \left(m_{\text{SM}}^2 + m_{\text{DM}}^2 + \frac{2m_{\text{SM}}m_{\text{DM}}}{\sqrt{1 - v_{\text{rel}}^2}} \right)^{1/2}. \quad (6)$$

For comparison purposes, the maximum mass splitting achieved by direct detection experiments and capture in neutron stars and white dwarfs is confronted with our results in Fig. 4. It can be clearly appreciated that for all DM masses, multimessenger observations of AGN allow us to reach larger mass splittings than complementary probes.

Discussions and implications. We have proposed a novel phenomenological probe of inelastic DM, relying on the

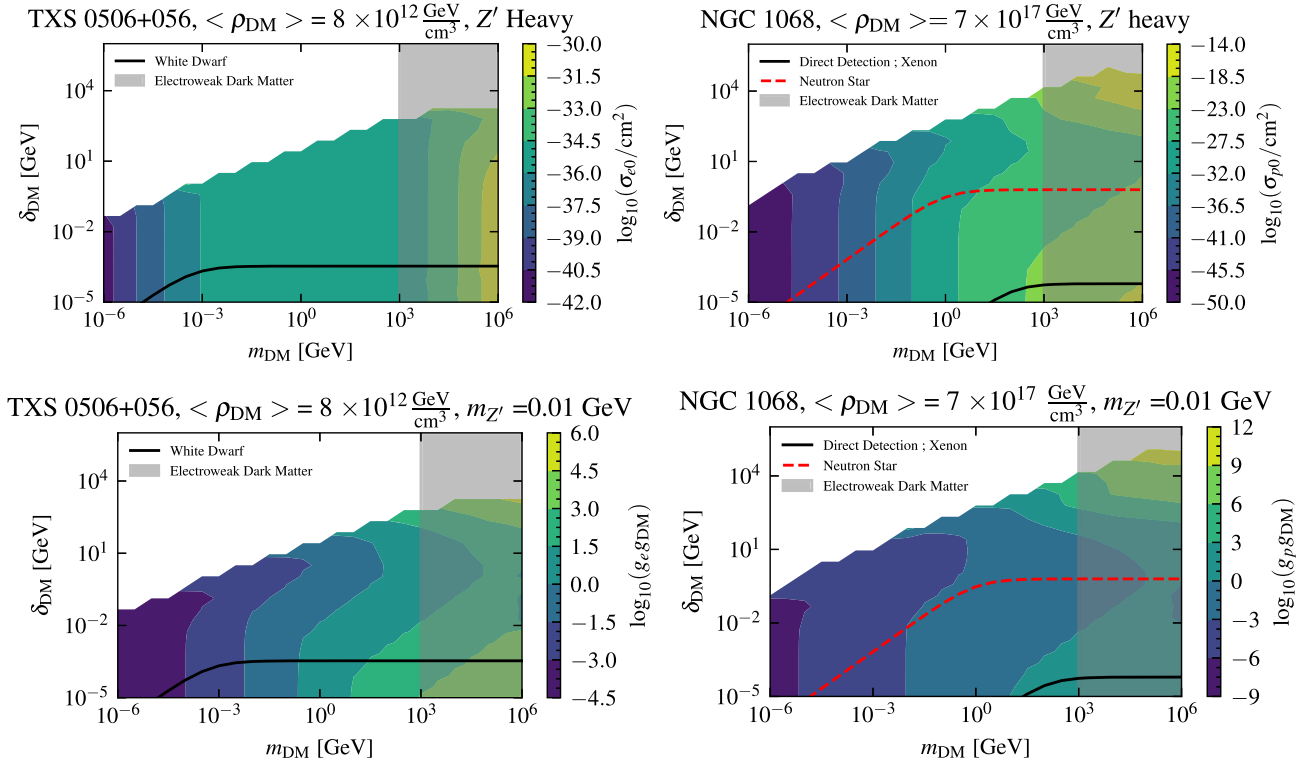


FIG. 4. Upper limits on (top) the characteristic scattering cross section given by Eq. (S7) [16] and (bottom) the product of DM and SM couplings to a vector mediator from the cooling of (left) electrons in TXS 056-0506 and (right) protons in NGC 1068 with a vector mediator. In the top plots, we consider a very heavy mediator (see Supplemental Material [16] where we comment on this further), while for the bottom plots we fix the mediator mass. Also included are lines for the maximal mass splitting able to be probed with direct detection and celestial bodies using Eq. (6) (direct detection is neglected for electrons, as the electron mass is too small for keV mass splitting with virialized DM). Finally, the region of $m_{\text{DM}} > 10^3$ GeV is shaded to indicate this region is of special interest for electroweak DM.

cooling of CRs in AGN through DM-proton and DM-electron upscatterings into an excited DM state. DM in the vicinity of NGC 1068 and TXS 0506 + 056 may scatter off CR protons and electrons, producing a heavier DM in the final state and cooling the CRs. Since CRs are responsible for the emission of high-energy neutrinos and gamma rays from these sources, observable on Earth, their cooling timescales would not be dominated by beyond the SM interactions; otherwise, such high-energy particle emission would be significantly depleted. The luminosity in protons and electrons in these sources is lower and upper bounded, which allows to quantify the uncertainties in the inferred cooling timescales within the SM, which are about one order of magnitude in NGC 1068 and TXS 0506 + 056.

A remarkable result of our work is the demonstration that CR cooling in AGN allows one to constrain unprecedentedly large mass splittings of inelastic DM particles, above the TeV scale. The cross sections constrained at those mass splittings, however, are larger than those expected in electroweakly interacting DM models. Such mass splittings are orders of magnitude larger than those probed by complementary astrophysical and laboratory searches, as highlighted in Fig. 1. Furthermore, for thermal light inelastic

DM, our cooling constraints can be comparable to or even overcome collider and beam-dump bounds for DM masses below $m_{\text{DM}} \leq 70$ MeV, probing thermal values.

The fact that DM direct detection experiments, gamma-ray, and neutrino telescopes have not found conclusive evidence for weakly interacting DM may indicate that the portal of the DM to the SM sector is more strongly suppressed than initially expected. The suppression may not occur at the level of the interaction probability but rather be purely kinematical. If the DM interacts only (or predominantly) inelastically with the SM sector, such process will only occur when the energy transfer of the scattering process exceeds the mass difference between the two DM states. If the mass splitting is sufficiently large, above a few GeV, the prospects for detection with traditional direct detection experiments or astrophysical probes such as neutron stars are not very promising. We have demonstrated that in those scenarios, CR accelerators like AGNs may still allow us to probe those models. A new frontier of inelastic DM with high mass splittings, above the TeV scale, has been opened.

Acknowledgments. We are grateful to Felix Kahlhoefer, Thomas Schwetz, and Giovanni Dalla Valle Garcia for

discussions on inelastic DM models. R. A. G., G. H., and I. M. S. are supported by the U.S. Department of Energy under Grant No. DE-SC0020262. M. M. and K. M. are supported by National Science Foundation (NSF) Grant No. AST-2108466. R. A. G. is partially supported by the World Premier International Research Center Initiative (WPI), Ministry of Education, Culture, Sports, Science and Technology (MEXT), Japan. R. A. G. is grateful to International Center for Quantum-field Measurement Systems for Studies of the Universe and Particles (QUP) for hospitality during his visit. G. H. and M. M. are grateful

to CERN for hospitality during their visit and partial support during the last stages of this work. M. M. also acknowledges support from the Institute for Gravitation and the Cosmos (IGC) Postdoctoral Fellowship. M. M. thanks the Galileo Galilei Institute for Theoretical Physics for the hospitality and the INFN for partial support during the completion of this work. The work of K. M. is supported by the NSF Grants No. AST-2108467 and No. AST-2308021 and KAKENHI No. 20H01901 and No. 20H05852.

-
- [1] A. M. Green, *SciPost Phys. Lect. Notes* **37**, 1 (2022).
 - [2] G. Bertone, D. Hooper, and J. Silk, *Phys. Rep.* **405**, 279 (2005).
 - [3] S. Profumo, L. Giani, and O. F. Piattella, *Universe* **5**, 213 (2019).
 - [4] M. Cirelli, A. Strumia, and J. Zupan, *arXiv:2406.01705*.
 - [5] M. W. Goodman and E. Witten, *Phys. Rev. D* **31**, 3059 (1985).
 - [6] A. K. Drukier, K. Freese, and D. N. Spergel, *Phys. Rev. D* **33**, 3495 (1986).
 - [7] L. J. Hall, T. Moroi, and H. Murayama, *Phys. Lett. B* **424**, 305 (1998).
 - [8] D. Tucker-Smith and N. Weiner, *Phys. Rev. D* **64**, 043502 (2001).
 - [9] N. Arkani-Hamed, D. P. Finkbeiner, T. R. Slatyer, and N. Weiner, *Phys. Rev. D* **79**, 015014 (2009).
 - [10] D. S. M. Alves, S. R. Behbahani, P. Schuster, and J. G. Wacker, *Phys. Lett. B* **692**, 323 (2010).
 - [11] S. Chang, N. Weiner, and I. Yavin, *Phys. Rev. D* **82**, 125011 (2010).
 - [12] N. Nagata and S. Shirai, *J. High Energy Phys.* **01** (2015) 029.
 - [13] N. Nagata and S. Shirai, *Phys. Rev. D* **91**, 055035 (2015).
 - [14] A. Filimonova, S. Junius, L. Lopez Honorez, and S. Westhoff, *J. High Energy Phys.* **06** (2022) 048.
 - [15] N. Brahma, S. Heeba, and K. Schutz, *Phys. Rev. D* **109**, 035006 (2024).
 - [16] See Supplemental Material at <http://link.aps.org/supplemental/10.1103/5m57-vgt2> contains further details on dark matter models, spike formation, and scattering.
 - [17] G. D. V. Garcia, F. Kahlhoefer, M. Ovchinnikov, and T. Schwetz, *J. High Energy Phys.* **02** (2025) 127.
 - [18] F. Kahlhoefer, K. Schmidt-Hoberg, T. Schwetz, and S. Vogl, *J. High Energy Phys.* **02** (2016) 016.
 - [19] M. Duerr, F. Kahlhoefer, K. Schmidt-Hoberg, T. Schwetz, and S. Vogl, *J. High Energy Phys.* **09** (2016) 042.
 - [20] T. Schwetz and J. Zupan, *J. Cosmol. Astropart. Phys.* **08** (2011) 008.
 - [21] J. Bramante, P. J. Fox, G. D. Kribs, and A. Martin, *Phys. Rev. D* **94**, 115026 (2016).
 - [22] M. Baryakhtar, A. Berlin, H. Liu, and N. Weiner, *J. High Energy Phys.* **06** (2022) 047.
 - [23] N. Song, S. Nagorny, and A. C. Vincent, *Phys. Rev. D* **104**, 103032 (2021).
 - [24] N. F. Bell, J. B. Dent, B. Dutta, S. Ghosh, J. Kumar, J. L. Newstead, and I. M. Shoemaker, *Phys. Rev. D* **104**, 076020 (2021).
 - [25] G. Herrera, A. Ibarra, and S. Shirai, *J. Cosmol. Astropart. Phys.* **04** (2023) 026.
 - [26] J. Eby, P. J. Fox, and G. D. Kribs, *J. High Energy Phys.* **06** (2024) 165.
 - [27] S. Chatterjee and R. Laha, *Phys. Rev. D* **107**, 083036 (2023).
 - [28] S. Kang, S. Scopel, and G. Tomar, *J. Cosmol. Astropart. Phys.* **01** (2025) 035.
 - [29] T. Emken, J. Frerick, S. Heeba, and F. Kahlhoefer, *Phys. Rev. D* **105**, 055023 (2022).
 - [30] R. Essig *et al.*, in Snowmass 2021, *arXiv:2203.08297*.
 - [31] Z. Yun, J. Sun, B. Zhu, and X. Liu, *Chin. Phys. C* **48**, 103106 (2024).
 - [32] J. Li, L. Su, L. Wu, and B. Zhu, *J. Cosmol. Astropart. Phys.* **04** (2023) 020.
 - [33] N. F. Bell, J. B. Dent, B. Dutta, J. Kumar, and J. L. Newstead, *Phys. Rev. D* **106**, 103016 (2022).
 - [34] Y. Gu, L. Wu, and B. Zhu, *Phys. Rev. D* **106**, 075004 (2022).
 - [35] N. F. Bell, G. Busoni, and S. Robles, *J. Cosmol. Astropart. Phys.* **09** (2018) 018.
 - [36] M. McCullough and M. Fairbairn, *Phys. Rev. D* **81**, 083520 (2010).
 - [37] D. Hooper, D. Spolyar, A. Vallinotto, and N. Y. Gnedin, *Phys. Rev. D* **81**, 103531 (2010).
 - [38] G. Alvarez, A. Joglekar, M. Phoroutan-Mehr, and H.-B. Yu, *Phys. Rev. D* **107**, 103024 (2023).
 - [39] B. Chauhan, M. H. Reno, C. Rott, and I. Sarcevic, *J. Cosmol. Astropart. Phys.* **01** (2024) 030.
 - [40] A. Biswas, A. Kar, H. Kim, S. Scopel, and L. Velasco-Sevilla, *Phys. Rev. D* **106**, 083012 (2022).
 - [41] M. Fujiwara, K. Hamaguchi, N. Nagata, and J. Zheng, *Phys. Rev. D* **106**, 055031 (2022).
 - [42] J. F. Acevedo, J. Bramante, Q. Liu, and N. Tyagi, *J. Cosmol. Astropart. Phys.* **03** (2025) 028.
 - [43] A. Berlin, G. Krnjaic, and E. Pinetti, *Phys. Rev. D* **110**, 035015 (2024).

- [44] A. Berlin, N. Blinov, G. Krnjaic, P. Schuster, and N. Toro, *Phys. Rev. D* **99**, 075001 (2019).
- [45] M. Mongillo, A. Abdullahi, B. B. Oberhauser, P. Crivelli, M. Hostert, D. Massaro, L. M. Bueno, and S. Pascoli, *Eur. Phys. J. C* **83**, 391 (2023).
- [46] G. Herrera and K. Murase, *Phys. Rev. D* **110**, L011701 (2024).
- [47] A. Ambrosone, M. Chianese, D. F. G. Fiorillo, A. Marinelli, and G. Miele, *Phys. Rev. Lett.* **131**, 111003 (2023).
- [48] F. M. Rieger, *Universe* **8**, 607 (2022).
- [49] K. Murase and F. W. Stecker, in *World Scientific Series in Astrophysics: The Encyclopedia of Cosmology* (2023), pp. 483–540, [10.1142/9789811282645_0010](https://doi.org/10.1142/9789811282645_0010).
- [50] K. Murase, S. S. Kimura, and P. Meszaros, *Phys. Rev. Lett.* **125**, 011101 (2020).
- [51] K. Murase, *Astrophys. J. Lett.* **941**, L17 (2022).
- [52] A. Keivani, K. Murase, M. Petropoulou, D. B. Fox, S. B. Cenko, S. Chaty, A. Coleiro, J. J. DeLaunay, S. Dimitrakoudis, P. A. Evans, J. A. Kennea, F. E. Marshall, A. Mastichiadis, J. P. Osborne, M. Santander, A. Tohuvavohu, and C. F. Turley, *Astrophys. J.* **864**, 84 (2018).
- [53] S. Sigurdsson, in *Carnegie Observatories Centennial Symposium. 1. Coevolution of Black Holes and Galaxies* (2003), [arXiv:astro-ph/0303311](https://arxiv.org/abs/astro-ph/0303311).
- [54] D. Merritt, M. Milosavljevic, L. Verde, and R. Jimenez, *Phys. Rev. Lett.* **88**, 191301 (2002).
- [55] D. Merritt, S. Harfst, and G. Bertone, *Phys. Rev. D* **75**, 043517 (2007).
- [56] G. Bertone, A. R. A. C. Wierda, D. Gaggero, B. J. Kavanagh, M. Volonteri, and N. Yoshida, [arXiv:2404.08731](https://arxiv.org/abs/2404.08731).
- [57] A. Das, B. T. Zhang, and K. Murase, *Astrophys. J.* **972**, 44 (2024).
- [58] J.-H. Woo and C. M. Urry, *Astrophys. J.* **579**, 530 (2002).
- [59] T. T. Ananna, C. M. Urry, E. Treister, R. C. Hickox, F. Shankar, C. Ricci, N. Cappelluti, S. Marchesi, and T. J. Turner, *Astrophys. J.* **903**, 85 (2020).
- [60] K. Murase, F. Oikonomou, and M. Petropoulou, *Astrophys. J.* **865**, 124 (2018).
- [61] E. Izaguirre, G. Krnjaic, and B. Shuve, *Phys. Rev. D* **93**, 063523 (2016).
- [62] M. C. González and N. Toro, *J. High Energy Phys.* **04** (2022) 060.